

*The Effect of Calcium Phosphate Hybridized Tendon Graft on Biomechanical Behavior
in Anterior Cruciate Ligament Reconstruction in a Goat Model: Novel Technique for
Improving Tendon-bone Healing*

Hiroataka Mutsuzaki¹, Masataka Sakane², Hiromichi Fujie³, Shinya Hattori⁴,
Hisatoshi Kobayashi⁴, and Naoyuki Ochiai²

¹Department of Orthopaedic Surgery, Ibaraki Prefectural University of Health Sciences,
4669-2 Ami, Ami-machi, Inashiki-gun, Ibaraki, 300-0394, Japan

² Department of Orthopaedic Surgery, Institute of Clinical Medicine,
Graduate School of Comprehensive Human Sciences, University of Tsukuba,
1-1-1 Tennodai, Tsukuba, Ibaraki, 305-8575, Japan

³ Division of Human Mechatronics Systems, Faculty of System Design,
Tokyo Metropolitan University,
6-6 Asahigaoka, Hino, Tokyo, 191-0044, Japan

⁴ Biomaterial Center, National Institute for Materials Science,
1-1 Namiki, Tsukuba, Ibaraki, 305-0044, Japan

Corresponding author:

Masataka Sakane, M.D., Ph.D.

E-mail address: sakane-m@md.tsukuba.ac.jp

Acknowledgements

The authors are grateful to Mr. Hitoshi Yagi in Kogakuin University for technical assistance. The authors thank the Leading Project (LP) of the Ministry of Education, Culture, Sports, Science and Technology of Japan for financial support.

Background: We developed a novel technique to improve tendon-bone attachment by hybridizing calcium phosphate (CaP) with a tendon graft using an alternate soaking process. However, the long-term result of the function of the anterior cruciate ligament (ACL) reconstructed knee and interface between the tendon and the bone is unclear.

Purpose: To clarify the effects of the CaP-hybridized tendon graft by analyzing the biomechanical behavior of the reconstructed knee, bone tunnel wall, and interface between the tendon and the bone compared with the untreated knee at 1 year in goats.

Study Design: Controlled laboratory study.

Methods: We analyzed knee kinematics and in situ forces in a replacement graft. Computed tomography (CT) for new bone formation in the bone tunnel, and histological analysis of the tendon-bone interface with and without the CaP-hybridized tendon graft were also analyzed.

Results: In the CaP group, the A-P translations in the reconstructed knees were shorter and the corresponding in situ forces were greater than those in the control group at full extension and 60° of knee flexion. The in situ force in response to applied internal tibial torques in the CaP group at full extension was greater than that in the control group. New bone formation in the bone tunnel and cartilage layer between the tendon-bone interface at the joint aperture site of the CaP group was more observed than that of the

control group.

Conclusions: The CaP-hybridized tendon graft promotes knee stability because of the firm tendon-bone healing with cartilage layer and new bone formation.

Clinical Relevance: ACL reconstruction using the CaP-hybridized tendon graft can lead to good long-term outcomes.

Key words:

ACL reconstruction, tendon-bone interface, calcium phosphate hybridization, biomechanical analysis

Introduction

An anterior cruciate ligament (ACL) is the most frequently injured ligament in the knee. Surgical reconstruction using a replacement graft is the preferred method of treatment. A semitendinosus-gracilis (STG) tendon graft, a soft tissue graft, is commonly used (14, 24). However, the STG tendon graft requires soft tissue-to-bone healing within bone tunnels. Grana et al. (6) showed indirect fibrous bonding at interface between hamstring tendon autograft and bone after ACL reconstruction in rabbits. Kurosaka et al. (11) also reported that the fixation site is mechanically the weakest link in any surgical techniques in the early postoperative period. Therefore, we developed a novel technique to improve tendon-bone attachment by hybridizing calcium phosphate (CaP) with tendons using an alternate soaking process (25). Using the CaP-hybridized tendon, we observed the direct-bonding area between the grafted tendon and the bone two to three weeks after ACL reconstruction in rabbits (17, 18) and also observed the direct-bonding area 6 weeks after the reconstruction in goats (16). The CaP-hybridized tendons enhance the proliferation of osteoclast-like cells and osteoblasts, which bond the implanted tendons to newly formed bone without inflammation and scar formation (17, 18). The long-term result of the function of the ACL reconstructed knee and interface between the CaP-hybridized tendon and the bone is not defined. We used a

goat model of ACL reconstruction to clarify this issue. Long-term studies using goat knees have shown the effective restoration of knee stability and minimal articular cartilage degeneration after ACL reconstruction (9, 19). Moreover, a goat model allows for more accurate and consistent surgical reconstruction than smaller animal models.

The objective of this study was to clarify the effects of the CaP-hybridized tendon graft by analyzing the knee kinematics of the reconstructed knee and in situ forces of the grafted tendon, dense bone formation around bone tunnels by computed tomography (CT) and interface between the grafted tendon and the bone by histological analysis compared with the untreated knee one year after the reconstruction in a goat model. We hypothesize that the kinematics and in situ forces of the reconstructed knee using a CaP-hybridized tendon graft are improved compared with those of an untreated tendon graft 1 year after reconstruction because of bone formation around the grafted tendon and improved tendon-bone interface.

Materials and Methods

CaP hybridization method

Eighteen skeletally mature female Saanen breed goats (50-70 kg) were used in this study (CaP, n = 6; control, n = 6; and intact-ACL, n = 6). The goats were

maintained in accordance with the guidelines of the Ethical Committee of the Biomaterial Center of the National Institute for Materials Science and the National Institute of Health guidelines for the care and use of laboratory animals (NIH Pub. No. 85-23 Rev. 1985).

Flexor digitorum longus (FDL) tendons and hamstring tendons were used in this study. Double-strand tendons of 45 mm length and 6.5 mm diameter were prepared. The tibial end of the grafts was secured using the Krackow technique with No. 2 nonabsorbable sutures (Ethibond* Excel, Ethicon, Inc., USA), and a polyester tape suture tied over the EndoButton[®] (Smith & Nephew, USA) was passed through the looped femoral end of the grafts. Then, the central third of the grafts, considered as the intra-articular portion, was covered with the sleeve of a rubber glove tied on each side with No. 2 nonabsorbable sutures to prevent soaking during CaP hybridization (Fig. 1a) (16). After these procedures, the CaP experimental grafts were soaked in 100 ml of a Ca solution (100 mM CaCl₂ + 30 mM L-histidine, pH 7.4, 280 mOsm/l) for 30 secs. The grafts were subsequently soaked in 100 ml of a NaHPO₄ solution (116.4 mM NaH₂PO₄:128.7 mM Na₂HPO₄·12H₂O = 15%:85%, pH 7.4, 280 mOsm/l) for 30 secs (Fig. 1b). The temperature of the solution and room was 25 °C. Before each soaking, the grafts were washed in a saline solution. This cycle was repeated ten times (16, 17, 18).

In a control experiment, the tendon was soaked in a saline solution for 10 min.

Surgical procedure

All the surgical procedures were performed under sterile conditions with the animals under general anesthesia. On the right knee, an anterior lateral skin incision was made. ACL was then completely transected, and gross anterior subluxation of the tibia was confirmed by manual examination. We drilled using a Kirschner wire from the anteromedial surface of the proximal tibia to the tibial insertion of the ACL. Then we drilled femoral side straightly with the knee positioned in 45° flexion to ensure consistency of surgical technique. The bone tunnel was reamed using a 6.5-mm-diameter canulated drill, resulting in the bone tunnel in the femoral side opening anterior of the femoral insertion. The length of the tunnel was at least 20 mm. The graft described above was passed through the femoral and tibial tunnels. The graft fixation was achieved via the EndoButton[®] at the femoral side and a 4.5-mm-diameter cortex screw (MEIRA Corporation, Nagoya, Japan) at the tibial side with 20 N as the initial tension (Fig. 1c) (16). We did not use double bundle grafts for the reconstruction to eliminate technical variables arising from multiple tunnel formation on a small bone.

Postoperatively, all the goats were allowed free activity in a cage (cage area,

50 square meters). Visual inspection revealed that normal gait patterns did not return until 3 to 4 weeks after surgery. The goats were sacrificed (1 ml of sodium pentobarbital per 4 kg goat mass administered intravenously) 52 weeks after surgery. A total of six specimens each from the CaP and control groups were obtained. The other six specimens were intact knee (intact-ACL group). The 18 specimens were sealed in double plastic bags and immediately stored at -20 °C until use for biomechanical analysis.

Biomechanical analysis

The robotic testing system simulator consisted of a 6-degrees-of-freedom (DOF) manipulator, servomotor controllers, and a control computer. The 6-DOF manipulator included a lower mechanism that moved in a translational axis and an upper mechanism that moved in two translational and three rotational axes. The femoral clamp was fixed to the lower mechanism, whereas the tibial clamp was fixed to the upper mechanism via a universal force/moment sensor (UFS) (UFS-45A50-U760/N, JR³ Inc., Woodland, Calif., USA) (Fig. 2). The robotic system was capable of controlling the displacement and force/moment applied to the knee in all 6 DOF based on a mathematical description of knee kinematics and kinetics (3, 5). Therefore, it was

possible to apply a single load or combined loads to the knee while still allowing natural joint motion using the system. In combination, this testing system enables the measurement of multiple-degrees-of-freedom knee kinematics and in situ forces in the ACL replacement graft when the knee is subjected to externally applied loads (12, 21, 22). The procedure of calculating and moving the manipulator was repeated at a rate of 300 to 500 milliseconds. The control and data acquisitions were performed using a personal computer in the C-language programming environment with a multitask operating system (CP/Q, IBM Japan, Kanagawa, Japan).

Before biomechanical analysis, each specimen was thawed for 24 hours at room temperature. The tibia and femur were cut 20 cm from the joint line, and the surrounding skin and muscles were dissected and removed 7 to 10 cm proximal and distal to the joint. To minimize bending or twisting during functional analysis, the specimens were potted in epoxy putty and secured with bolts in 6-mm-thick plastic cylinders. A specimen was first fixed to the simulator using the locations of the femoral insertion sites of the medial and lateral collateral ligaments as positioning datum points. The specimens were kept moist with 0.9% saline solution throughout dissection and biomechanical analysis. To identify the neutral position of the knee, the path of passive flexion-extension of the joint from full extension to 90° of knee flexion was first

determined by the robotic/UFS testing system in the force-control mode. The starting points for the application of external loads were determined throughout the range of flexion at a position where all external forces and moments in the joint were minimized. After determining the path of passive flexion-extension of the reconstructed knee, the robotic/UFS testing system was used in the force-control mode to determine the 5-DOF knee kinematics in response to a 50 N anterior-posterior (A-P) tibial load and 2.0 Nm internal tibial torque at fixed knee flexion angles of full extension, and 60° and 90° of knee flexion (8, 13, 21). The three-dimensional path of the knee motion was recorded over all five cycles, and the 6-DOF forces/moments on the knee were recorded in the fifth cycle that is considered original knee motion. After the ACL and ACL graft was transected near its tibial insertion site, the simulator reproduced the identical three-dimensional paths of the knee motion before transected while measuring the 6-DOF forces/moments on the knee during the fifth cycle. The in situ force in the ACL and ACL graft during the flexion-extension, A-P drawer tests, and internal tibial rotation tests was calculated from the difference in force/moment during the fifth cycle between the untransected and the transected knee using the principle of superposition (4). We used the data of the intact-ACL as the reference values.

CT analysis

After biomechanical analysis, CT of the specimens in the CaP and control group was performed (La Theta LCT-100, ALOKA CO., LTD., Tokyo, Japan) in the full extension of knee position for analyzing the difference in new bone formation (high density area) in the wall of bone tunnel. Axial images for a bone axis were obtained in both the femur and tibia 5 mm near the joint. The percentage of the new bone formation in the wall of bone tunnel was measured. They were blinded by an orthopedic surgeon.

Histological analysis

After CT, the specimens in the CaP group and control group were subjected to histological analysis. The femur-ACL graft and ACL graft-tibia complex were harvested. The specimens were fixed in 10% neutral-buffered formalin, decalcified, and embedded in paraffin. The specimens were sliced 5 μ m thick sagittal to the bone tunnel. Hematoxylin and eosin (H-E), safranin-O staining for the identification of the cartilage layer in the interface, and Masson's trichrome (MT) staining for the identification of collagenous fiber tissue were performed. The specimens were examined by light microscopy after staining. Histological comparisons of the tendon-bone interface (femoral and tibial side, and cartilaginous insertion or fibrous insertion) and grafted

tendon at the intra-articular portion were carried out between the CaP group and control. Moreover, the length and the width of the red stained area by safranin-O staining in cartilage layer at the anterior and posterior interface in both femur and tibia were measured. They were blinded by an orthopedic surgeon.

Statistical Analyses

To examine the average full extension angle of knees in the CaP, control, and intact-ACL groups, a one-way analysis of variance (ANOVA) was performed. The obtained biomechanical data, CT analysis and histological analysis were compared using Student's *t*-test at a $p < 0.05$ significance value.

Results

Biomechanical analysis

All ACL replacement grafts were intact at 52 weeks. The biomechanical data (CaP, $n = 6$; control, $n = 6$; and intact-ACL, $n = 6$) in response to a 50 N applied A-P tibial load are shown in Tables 1 and 2. The average full extension angles of knees in the CaP, control, and intact-ACL groups were $40.8 \pm 7.0^\circ$, $34.2 \pm 10.2^\circ$, and $35.2 \pm 4.7^\circ$, respectively. There was no significant difference ($p = 0.300$).

The A-P translation in the reconstructed knees in the CaP group were significantly smaller than those in the control group at full extension ($p = 0.034$) and 60° of knee flexion ($p = 0.009$). At a flexion angle of 90° , there was no significant difference between the control and CaP groups ($p = 0.381$). The A-P translation in the intact-ACL group was significantly smaller than those in the CaP ($p = 0.002$) and control ($p < 0.001$) groups at full extension. The A-P translation in the intact-ACL group at 60° of knee flexion was significantly smaller than that in the control ($p = 0.004$) group, but not significantly different from that in the CaP ($p = 0.159$) group. The A-P translation at 90° of knee flexion in the intact-ACL group was not significantly difference between the CaP ($p = 0.148$) and the control ($p = 0.139$) groups.

The corresponding in situ forces in the CaP group were greater than those in the control group at full extension ($p = 0.005$) and 60° ($p = 0.005$) of knee flexion, but not significantly different from that at 90° ($p = 0.232$). The in situ forces in the intact-ACL group at full extension and 60° of knee flexion were significantly greater than those in the control ($p = 0.002$ and $p < 0.001$, respectively), and that at 60° of knee flexion in the intact-ACL group was significantly greater than in the CaP group ($p = 0.023$), but not significantly different from that at full extension in the CaP group ($p = 0.112$). The in situ force in the intact-ACL group at 90° of knee flexion was

significantly greater than that in the control group ($p = 0.021$), but not significantly difference from that in the CaP group ($p = 0.080$).

The biomechanical data (CaP, $n = 6$; control, $n = 6$; and intact-ACL, $n = 6$) in response to a 2.0 Nm applied internal tibial torque is shown in Tables 3 and 4. One of the six specimens at 90° of knee flexion in the control and intact-ACL groups could not be analyzed, because the rotation angle was so large that the arms of the robot clashed with each other.

The internal tibial rotation angle in the control group was not significantly different from those in the CaP group at full extension ($p = 0.380$), 60° ($p = 0.107$), and 90° of knee flexion ($p = 0.289$). The internal tibial rotation angles in the intact-ACL group at full extension, 60°, and 90° of knee flexion were significantly greater than those in the CaP ($p = 0.027$, $p = 0.009$ and $p = 0.011$, respectively) and control ($p = 0.004$, $p < 0.001$ and $p = 0.027$, respectively) groups.

The corresponding in situ force in the CaP group was greater than that in the control group at full extension ($p = 0.012$) but not significantly different at 60° ($p = 0.052$) and 90° ($p = 0.270$) of knee flexion. The in situ forces in the intact-ACL group at full extension and 60° of knee flexion were significantly greater than those in the CaP ($p < 0.001$ and $p = 0.004$, respectively) and the control ($p < 0.001$ and $p < 0.001$,

respectively) groups, but not significantly different at 90° ($p = 0.425$ and $p = 0.245$, respectively) of knee flexion.

CT analysis

The CT analysis is shown in Table 5. The percentage of new bone formation in femoral ($96.0 \pm 3.2\%$, $p = 0.005$) and tibial bone tunnel ($94.5 \pm 6.5\%$, $p < 0.001$) in the CaP group were significantly greater than that in the control group (femoral: $54.4 \pm 32.4\%$ and tibial: $44.4 \pm 21.9\%$, respectively). Moreover, the bony septum in the bone tunnel was observed in 1 of 6 specimens of femoral and tibial bone tunnels (Fig. 3). This indicates bone formation around double-strand tendon grafts.

Histological analysis

In the CaP-hybridized tendon grafts, the formation of a direct bond between the tendon and the bone was observed in femoral and tibial bone tunnels. In femoral and tibial bone tunnel at the anterior and posterior of the joint aperture site, cartilage layers with glycosaminoglycan stained by safranin-O were observed (Fig. 4). At the joint aperture site, cartilage layers between the tendon and the bone were observed at the anterior surface of the tibial bone tunnel in 5 of 6 specimens, at the posterior surface of

the tibial bone tunnel in 5 of 6 specimens, at the anterior surfaces of the femoral bone tunnel in 3 of 6 specimens, and at the posterior surface of the femoral bone tunnel in 6 of 6 specimens.

In the control group, the fibrous connective tissue between the grafted tendon and the bone interface was observed (Fig. 5). Sharpey's fibers-like tissue penetrated the bone, as shown by MT staining. The cartilage layer at the interface in control group was observed at the anterior surface of the tibial bone tunnel in 2 of 6 specimens, at the posterior surface of the tibial bone tunnel in 3 of 6 specimens, at the anterior surfaces of the femoral bone tunnel in 2 of 6 specimens, and at the posterior surface of the femoral bone tunnel in 1 of 6 specimens. The cartilage layers formed near the joint observed at the interface between the tendon and the bone in the CaP group were larger than those in the control group. The length and width at posterior femoral interface of red stained area by Safranin-O staining in cartilage layer in the CaP group were greater than that in the control ($p = 0.009$ and $p = 0.015$, respectively) (Table 6). The length at anterior tibial interface and width at posterior tibial interface of the red stained area in the CaP group were greater than that in the control ($p = 0.045$ and $p = 0.034$, respectively) (Table 6).

In both reconstructed groups, ACL grafts showed distinguishable collagen fibers with a crimp pattern, sparse spindle-shaped cells, and well-defined blood vessels

throughout the tissue. Additionally, no signs of necrosis were evident at 52 weeks (Fig. 6).

Discussion

The CaP hybridization technique is a simple method, is safe for the living tissue, and requires inexpensive materials. Moreover, we can hybridize CaP to desirable soft tissue areas intraoperatively in the operating room by the surgeon (e.g., ACL graft, rotator cuff, and flexor tendon for not only autograft but also allograft).

Although the knee kinematics and in situ forces of the ACL reconstructed knee in animals study were inferior to those in humans cases, both knee kinematics and in situ forces of ACL determined using a robotic-UFS system provide us detailed information (13). We also use the data from the biomechanical analysis of intact-ACL as the target values for the reconstructed knees.

The AP translation at full extension in the CaP group was greater than that in the intact-ACL group. However, the in situ force at full extension in the CaP group was not significantly different from that in the intact-ACL group. Because the knee kinematics differ for each knee angle and is affected by differences in surrounding tissues (osteoarthritis and contracture) between normal knee and reconstructed knee

after 1 year, the in situ force of the ligament may be more important for evaluating the biomechanical properties of the grafted tendon than the knee kinematics at full extension. The AP translation at 60° of knee flexion in the CaP group was not significantly different from that in the intact-ACL group. However, the in situ force at 60° of knee flexion in the CaP group was smaller than that in the intact-ACL. In the CaP group, the A-P translations were shorter and in situ force at full extension and 60° of knee flexion were greater than those in the control group. Moreover, the knee kinematics and in situ force in the CaP group were closer to those in the intact-ACL group than in the control group, even 1 year after ACL reconstruction. Therefore, the CaP-hybridized tendon graft promotes more knee stability than the graft in the control group 1 year after ACL reconstruction. Because the CaP-hybridized tendon graft enhanced bone formation and tendon-bone healing near to the joint aperture of the femoral and tibial bone tunnels as compared with the case of the control, the length of the CaP-hybridized tendon between the bone anchoring points of the femoral and tibial side can be shorter than that of untreated tendon. Therefore, knee stability and effective tensile stress in the CaP-hybridized tendon graft can be maintained (8). Moreover, the attachment area between the CaP-hybridized tendon graft and the bone can be larger than that in the case of the control near the joint line. Therefore, the in situ force at

applied internal tibial torque at full extension in the CaP group could be larger than that in the control group, even in the case of one-bundle ACL reconstruction. The appearance of the grafted tendons in both the CaP and control group were similar to each other. Therefore, the improved knee function in the CaP group compared with the control group can result in firm anchoring between the grafted tendon and the bone rather than in increasing grafted tendon strength.

Although two definite cartilage layers were not observed in any specimens in our study, the cartilage layer stained red by safranin-O staining at the interface in the femoral side at the posterior of the joint aperture site and the tibial side at the anterior and posterior of the joint aperture site in the CaP group was observed to be more distinct than that in the control group (Table 6). Tensile stress and/or compressive stress at the interface can promote the formation of the cartilage layer after the layer directly bonded with the bone tunnel in the CaP group (16, 17, 18). On the other hand, shear stress between the grafted tendon and the bone associated with the bungee effect (7) can form fibrous tissue at the interface in the control group, as previously reported (6, 18). ACL insertion consists of four distinguishable tissue layers of transition, that is, the ligaments, fibrocartilage, mineralized fibrocartilage, and bone (1, 2). The fibrocartilage and mineralized cartilage function as stress or shock absorbers by reducing the stiffness

gradient between the ligament and the bone (10, 23). Reconstructing the highly specialized structure of a cartilaginous insertion is necessary for normal ligament function (15), because cartilaginous insertions serve to compensate for the various elastic modules of the ligament and bone (10). No difference was observed in the length and width of the stained layer of cartilage between the CaP group and the control group at the interface in the anterior femoral side, because this area experiences more graft tunnel motion (shear stress) than the other area. Therefore, appropriate mechanical stress could not act between the CaP-hybridized tendon graft and the bone at the interface in the anterior femoral side. We considered that appropriate mechanical stress at the interface after bonding between tendon graft and bone, and prerequisite firm anchoring for maturation of grafted tendon would be important. The midsubstance of the graft using the CaP-hybridization method may lead to regaining mechanical strength due to its effective load transfer through the tibia-graft-femur construct after anchoring.

The walls of bone tunnel in the CaP group showed more new bone formation than those in the control group. New bone formation in the bone tunnel of the CaP group was more vigorous than that in the control (16, 17, 18). The new bone formation area can be the direct bonding area between the grafted tendon and the bone. The new bone formation can prevent knee instability associated with bone tunnel enlargement.

Enlargement of the articular end of the bone tunnels owing to bone resorption is a common problem in ACL reconstruction (20). We considered that the new bone formation in the CaP group was effective for the long-term knee function by preventing instability associated with bone tunnel enlargement.

As described in the hypothesis, the kinematics and in situ forces of the reconstructed knee using a CaP-hybridized tendon graft were improved compared with those of an untreated tendon graft 1 year after reconstruction because of new bone formation around the grafted tendon and improved tendon-bone interface with cartilage layer near the joint.

A limitation of this study was that we could not perform a combined load test such as the pivot-shift test. Since the knee extension of goat is approximately – 30 degree, it is difficult to apply the pivot-shift maneuver. Moreover, we could not perform a load-to-failure analysis, because we had to cut the graft to measure the in situ force on the implanted graft using the robotic test. Results in animal studies may differ from those in humans, as it is difficult to set appropriate conditions for ACL reconstruction by joint geometry. However, we consider that the data using the robotic test is important in predicting the knee function of the reconstructed knee after 1 year.

Clinically, human ACL reconstruction after 1 year is a generally important

period for returning to sports. The CaP-hybridized tendon graft promotes knee stability because of the firm tendon-bone healing with cartilage layer. Therefore, the ACL reconstruction using the CaP-hybridized tendon graft can lead to long-term good results without knee instability associated with the loosening of the bone-tendon junction and bone tunnel enlargement. Presently, we are conducting a clinical study comparing CaP hybridizing methods with a conventional technique.

References

- (1) Benjamin M, Evans EJ, Copp L. The histology of tendon attachments to bone in man. *J Anat.* 1986;149:89-100.
- (2) Cooper RR, Misol S. Tendon and ligament insertion: a light and electron microscopic study. *J Bone Joint Surg Am.* 1970;52:1-20.
- (3) Fujie H, Livesay GA, Fujita M, Woo SL. Forces and moments in six-DOF at the human knee joint: mathematical description for control. *J Biomech.* 1996;29:1577-1585.
- (4) Fujie H, Livesay GA, Woo SL, Kashiwaguchi S, Blomstrom G. The use of a universal force-moment sensor to determine in-situ forces in ligaments: a new methodology. *J Biomech Eng.* 1995;117:1-7.
- (5) Fujie H, Mabuchi K, Woo SL, Livesay GA, Arai S, Tsukamoto Y. The use of robotics technology to study human joint kinematics: a new methodology. *J Biomech Eng.* 1993;115:211-217.
- (6) Grana WA, Egle DM, Mahnken R, Goodhart CW. An analysis of autograft fixation after anterior cruciate ligament reconstruction in a rabbit model. *Am J Sports Med.* 1994;22:344-351.
- (7) Höher J, Livesay GA, Ma CB, Withrow JD, Fu FH, Woo SL. Hamstring graft

motion in the femoral bone tunnel when using titanium button/polyester tape fixation.

Knee Surg Sports Traumatol Arthrosc. 1999;7:215-219.

(8) Ishibashi Y, Rudy TW, Livesay GA, Stone JD, Fu FH, Woo SL. The effect of anterior cruciate ligament graft fixation site at the tibia on knee stability: Evaluation using a robotic testing system. *Arthroscopy*. 1997;13:177-182.

(9) Jackson DW, Grood ES, Goldstein JD, Rosen MA, Kurzweil PR, Cummings JF, Simon TM. A comparison of patellar tendon autograft and allograft used for anterior cruciate ligament reconstruction in the goat model. *Am J Sports Med*. 1993;21:176-185.

(10) Knese K-H, Biermann H. Die Knochenbildung an Sehnen und Bandansätzen im Bereich ursprünglich chondraler Apophysen. *Z Zellforsch*. 1958;49:142-187.

(11) Kurosaka M, Yoshiya S, Andrish JT. A biomechanical comparison of different surgical techniques of graft fixation in anterior cruciate ligament reconstruction. *Am J Sports Med*. 1987;15:225-229.

(12) Livesay GA, Fujie H, Kashiwaguchi S, Morrow DA, Fu FH, Woo SL. Determination of the in-situ forces and force distribution within the human anterior cruciate ligament. *Ann Biomed Eng*. 1995;23:467-474.

(13) Ma CB, Papageorgiou CD, Debski RE, Woo SL. Interaction between the ACL graft and MCL in combined ACL+MCL knee injury using a goat model. *Acta Orthop Scand*.

2000;71:387-393.

(14) Maeda A, Shino K, Horibe S, Nakata K, Buccafusca G. Anterior cruciate ligament reconstruction with multistranded autogenous semitendinosus tendon. *Am J Sports Med.* 1996;24:504-509.

(15) Messner K. Postnatal development of the cruciate ligament insertions in the rat knee. *Acta Anat (Basel).* 1998;160:261-268.

(16) Mutsuzaki H, Sakane M, Hattori S, Kobayashi H, Ochiai N. Firm Anchoring between Calcium Phosphate-Hybridized Tendon and Bone for Anterior Cruciate Ligament Reconstruction in a Goat Model. *Biomed Mater.* 2009;4:045013(7pp).

(17) Mutsuzaki H, Sakane M, Ito A, Nakajima H, Hattori S, Miyanaga Y, Tanaka J, Ochiai N. The interaction between osteoclast-like cells and osteoblasts mediated by nanophase calcium phosphate-hybridized tendons. *Biomaterials.* 2005;26:1027-1034.

(18) Mutsuzaki H, Sakane M, Nakajima H, Ito A, Hattori S, Miyanaga Y, Ochiai N, Tanaka J. Calcium-phosphate-hybridized tendon directly promotes regeneration of tendon-bone insertion. *J Biomed Mater Res A.* 2004;70:319-327.

(19) Ng GY, Oakes BW, Deacon OW, McLean ID, Lampard D. Biomechanics of patellar tendon autograft for reconstruction of anterior cruciate ligament in the goat: Three-year study. *J Orthop Res.* 1995;13:602-608.

- (20) Rodeo SA, Kawamura S, Ma CB, Deng XH, Sussman PS, Hay P, Ying L. The effect of osteoclastic activity on tendon-to-bone healing: an experimental study in rabbits. *J Bone Joint Surg Am.* 2007;89:2250-2259.
- (21) Rudy TW, Livesay GA, Woo SL-Y, Fu FH. A combined robotic/universal force sensor approach to determine in situ forces of knee ligaments. *J Biomech.* 1996;29:1357-1360.
- (22) Sakane M, Fox RJ, Woo SL-Y, Livesay GA, Li G, Fu FH. In situ forces in the anterior cruciate ligament and its bundles in response to anterior tibial loads. *J Orthop Res.* 1997;15:285-293.
- (23) Schneider H. Zur Struktur der Sehnenansatzzonen. *Z Anat.* 1956;119:431-456.
- (24) Swenson TM, Harner CD, Fu FH. Endoscopic ACL reconstruction using a quadrupled semitendinosus graft. *Pittsburgh Orthop J.* 1995;6:25-33.
- (25) Taguchi T, Kishida A, Akashi M. Hydroxyapatite formation on/in hydrogels using a novel alternate soaking process. *Chem Lett.* 1998;8:711-712.

Figure legends

Figure 1.

(a) Masking technique

The central third of the grafts, considered as the intra-articular portion, was covered with the sleeve of a rubber glove tied on each side to prevent CaP hybridization.

(b) CaP hybridization method

Ca = calcium solution, S = saline solution, P = NaHPO₄ solution

The tendon graft was soaked in a calcium solution solution for 30 secs. The grafts were subsequently soaked in a NaHPO₄ solution for 30 secs. Before each soaking, the grafts were washed in a saline solution.

(c) ACL reconstruction

The graft (black arrow) was pulled taut through the drill hole with both ends fixed at the distal part of the femur (EndoButton) and proximal part of the tibia (screw).

Figure 2.

Photograph of a specimen mounted on the robotic/UFS testing system. (A) 6 degrees of freedom; (B) Tibia fixed in tibial clamp; (C) UFS; (D) Femur mounted in femoral clamp.

Figure 3.

CT images of bone tunnel wall of femur

(a): In the CaP group, distinct bone formation around the wall of the bone tunnel, and the bone septum in the bone tunnel was observed.

(b): In the control, the bone formation of the wall of the bone tunnel was slight.

Figure 4.

Histological sections by safranin-O staining in CaP group in femur.

(a) low magnified image (x 12.5), (b) square area of (a) image (x 100), (c) square area of (b) image (x 400).

T = tendon graft, B = bone, C = cartilage tissue, Ant = anterior, Post = posterior, Prox = proximal, Dist = distal

A cartilage layer stained red by glycosaminoglycan was observed between the grafted tendon and the bone at posterior of joint aperture site in femur.

Figure 5.

Histological sections by safranin-O staining in control group in femur.

(a) low magnified image (x 12.5), (b) square area of (a) image (x 100), (c) square area of (b) image (x 400).

T = tendon graft, B = bone, F = fibrous tissue, Ant = anterior, Post = posterior, Prox = proximal, Dist = distal

A cartilage layer stained red by glycosaminoglycan was not observed at the interface.

Fibrous connective tissue (Sharpey's fibers-like tissue) was observed at the interface.

Figure 6.

Histological sections of ACL grafts that were in intraarticular portion.

H-E staining (x 100)

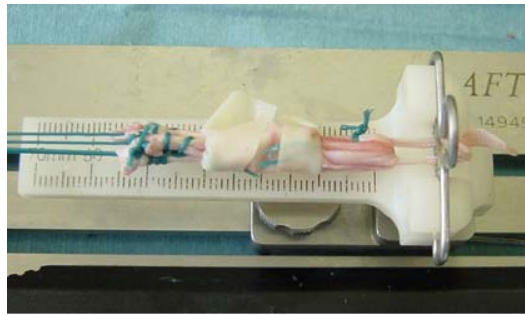
(a): CaP hybridized tendon graft

(b) untreated tendon graft

In both group, ACL grafts showed distinguishable collagen fibers with a crimp pattern, sparse spindle-shaped cells, and well-defined blood vessels throughout the tissue at 52 weeks.

Figure

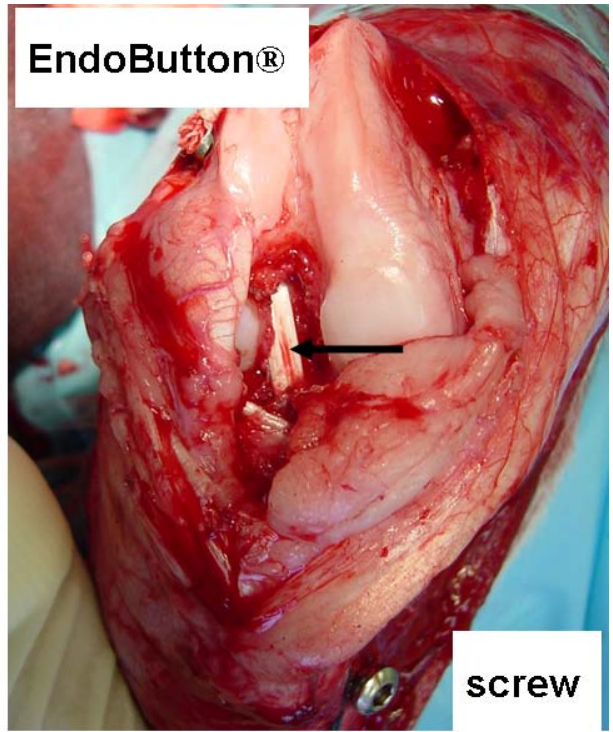
Figure 1.



(a)



(b)



(c)

Figure 2.

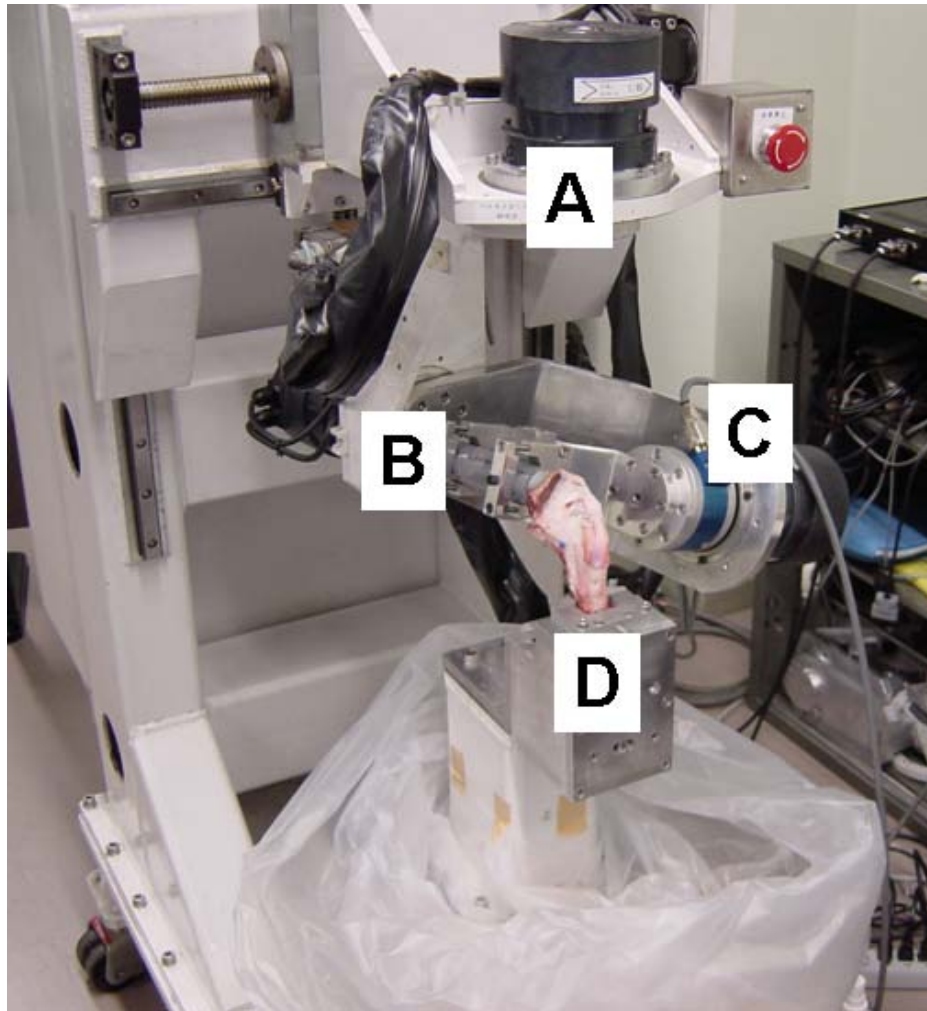
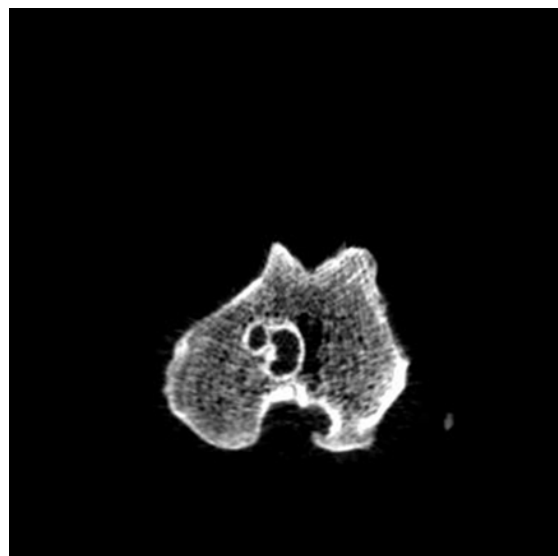
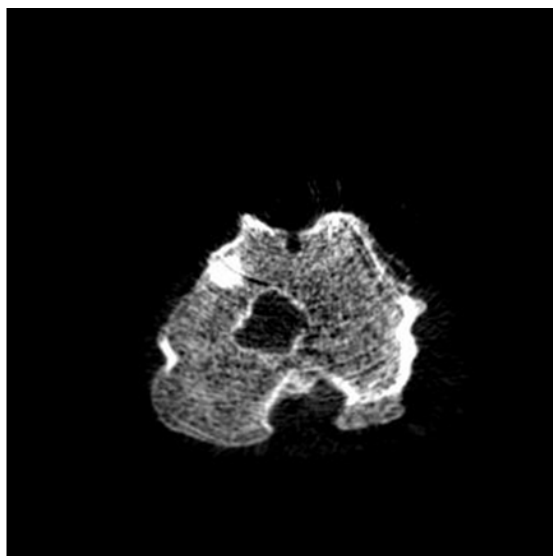


Figure 3.



(a)



(b)

Figure 4.

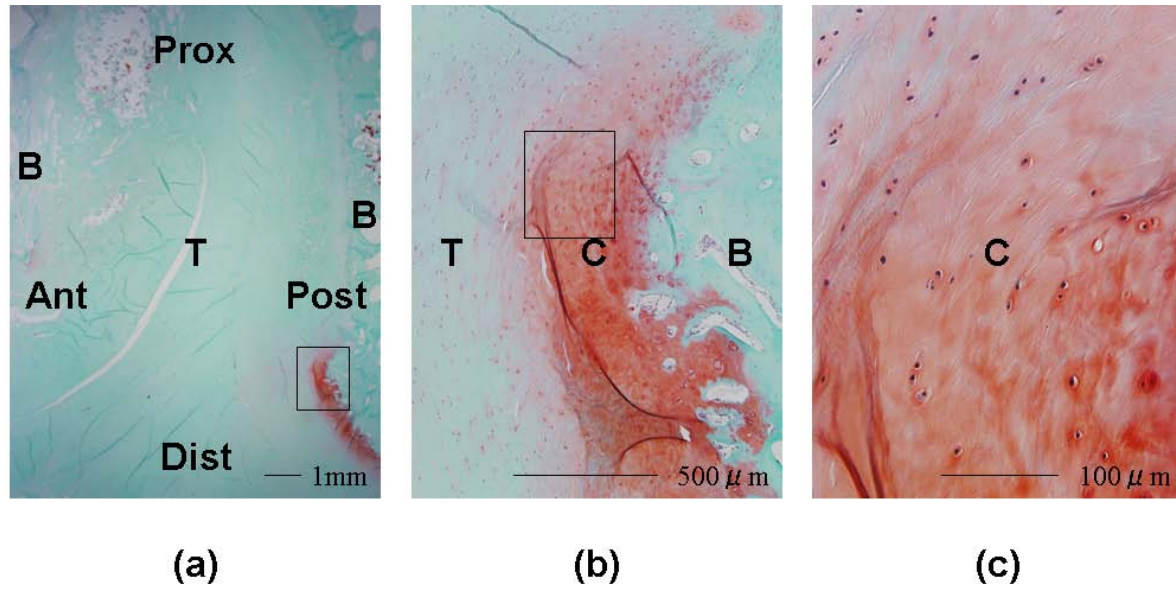


Figure 5.

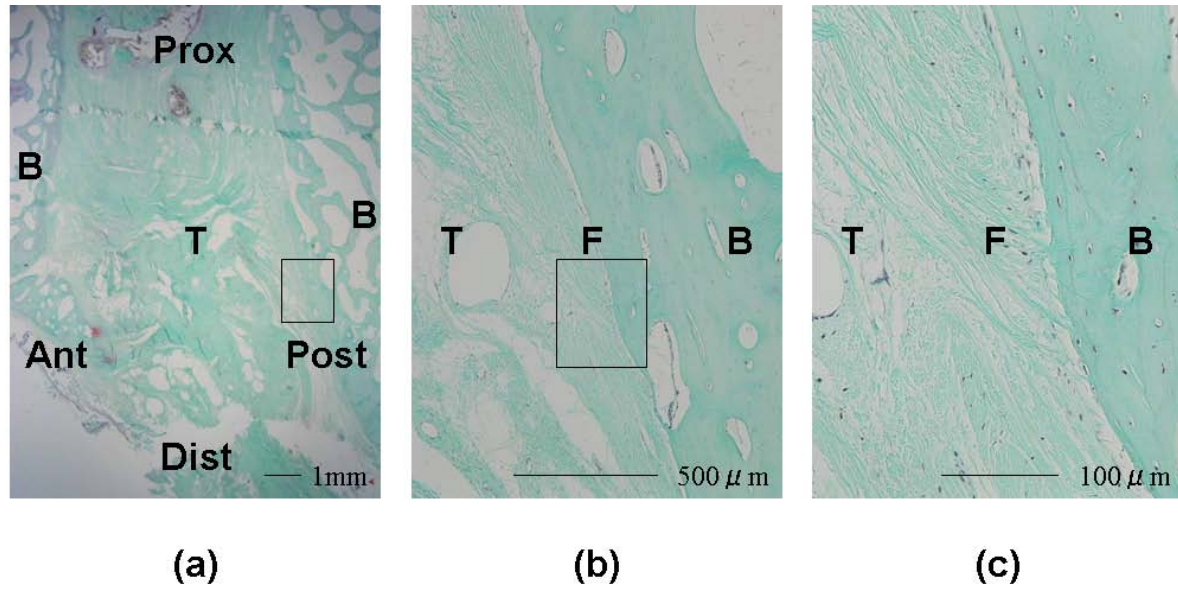
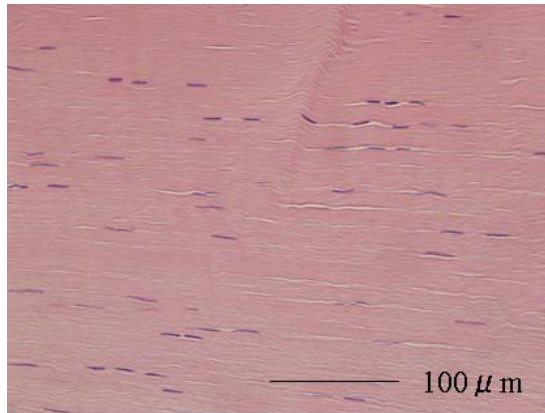
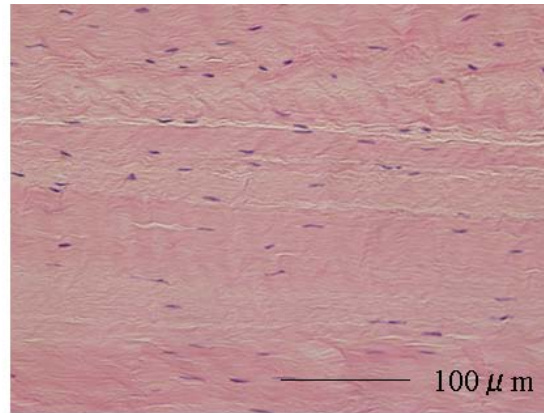


Figure 6.



(a)



(b)

Table 1: Total AP tibial translation in response to a 50-N AP tibial load for the intact-ACL, CaP and control groups at 1 year (mean \pm SD)

Knee flexion	Total AP tibial translation (mm)		
	Intact-ACL (n = 6)	CaP (n = 6)	Control (n = 6)
full extension	0.9 \pm 0.1 a, c	3.8 \pm 1.8 a, b, c	6.1 \pm 2.1 b, c
60°	5.8 \pm 1.9 a, c	6.8 \pm 1.4 a, c	8.7 \pm 1.0 b, c
90°	12.2 \pm 2.9 c	10.8 \pm 1.4 c	10.4 \pm 2.5 c

a: $p < 0.05$ compared with control values.

b: $p < 0.05$ compared with intact-ACL values.

c: $p < 0.05$ compared within each group values.

Table 2: In situ force in the ACL and ACL graft in response to a 50-N AP tibial load for the intact-ACL, CaP and control groups at 1 year (mean \pm SD)

Knee flexion	In situ force in the graft (N)		
	Intact-ACL (n = 6)	CaP (n = 6)	Control (n = 6)
full extension	53.8 \pm 12.8 a	45.8 \pm 7.9 a, c	23.9 \pm 14.7 b
60°	48.4 \pm 14.0 a	33.7 \pm 7.2 a, b, c	16.3 \pm 11.2 b
90°	41.7 \pm 20.6 a	25.4 \pm 16.4 c	19.1 \pm 11.3 b

a: $p < 0.05$ compared with control values.

b: $p < 0.05$ compared with intact-ACL values.

c: $p < 0.05$ compared within each group values.

Table 3: Internal tibial rotation in response to a 2.0-Nm internal tibial torques for the intact-ACL, CaP and control groups at 1 year (mean \pm SD)

Knee flexion	Internal tibial rotation ($^{\circ}$)		
	Intact-ACL (n = 6)	CaP (n = 6)	Control (n = 6)
full extension	51.4 \pm 6.7 a, c	31.7 \pm 7.5 b, c	33.4 \pm 11.3 b, c
60 $^{\circ}$	53.4 \pm 7.6 a	35.4 \pm 15.4 b	45.0 \pm 8.9 b, c
90 $^{\circ}$	61.4 \pm 7.1 (n = 5) a, c	44.5 \pm 5.7 b, c	47.0 \pm 8.8 (n = 5) b, c

a: $p < 0.05$ compared with control values.

b: $p < 0.05$ compared with intact-ACL values.

c: $p < 0.05$ compared within each group values.

Table 4: In situ force in the ACL and ACL graft in response to a 2.0-Nm internal tibial torques for the intact-ACL, CaP and control groups at 1 year (mean \pm SD)

Knee flexion	In situ force in the graft (N)		
	Intact-ACL (n = 6)	CaP (n = 6)	Control (n = 6)
full extension	69.3 \pm 6.5 a, c	23.1 \pm 2.6 a, b	14.7 \pm 7.3 b
60°	43.0 \pm 15.4 a, c	19.2 \pm 8.6 b	11.8 \pm 5.2 b
90°	23.5 \pm 19.3 (n = 5) c	26.9 \pm 35.0	16.6 \pm 8.8 (n = 5)

a: $p < 0.05$ compared with control values.

b: $p < 0.05$ compared with intact-ACL values.

c: $p < 0.05$ compared within each group values.

Table 5: CT evaluation: Percentage of new bone formation in bone tunnel

	Femoral side (%)	Tibial side (%)
CaP group (n = 6)	96.0 ± 3.2 *	94.5 ± 6.5 *
Control (n = 6)	54.4 ± 32.4	44.4 ± 21.9

Results are the mean ± SD

* p < 0.05 compared with control values.

Table 6: Histological analysis: Red stained area by Safranin-O staining in cartilage layer at interface

	Femoral side				Tibial side			
	anterior		posterior		anterior		posterior	
	length (mm)	width (mm)	length (mm)	width (mm)	length (mm)	width (mm)	length (mm)	width (mm)
CaP group (n = 6)	0.83 ± 0.98	0.42 ± 0.55	1.88 ± 1.23 *	0.56 ± 0.41 *	1.47 ± 1.04 *	0.67 ± 0.43	2.85 ± 2.51	1.05 ± 0.72 *
Control (n = 6)	0.73 ± 0.88	0.19 ± 0.22	0.26 ± 0.65	0.08 ± 0.21	0.48 ± 0.75	0.25 ± 0.42	1.63 ± 1.51	0.41 ± 0.27

Results are the mean ± SD

* p < 0.05 compared with control values.